Scilight

Complex Systems Stability & Control
https://www.sciltp.com/journals/cssc

Article

Check for updates

Sampled-Data Control of Networked Autonomous Spacecraft under Sporadic Measurement

Yingwei Deng [1], Nanjun Ye [1], Hao Yan [2,*], Hui Shao [1,*], Ying Zhao [1] and Kui Ding [1]

[1] Key Laboratory of Advanced Perception and Intelligent Control of High-End Equipment, Ministry of Education, Anhui Polytechnic University, Wuhu 241000, China
[2] School of Mathematics and Statistics, Anhui Normal University, Wuhu 241000, China
* Correspondence: haoyan99183@163.com (H.Y.); 19142416991@163.com (H.S.)

How To Cite: Deng, Y.; Ye, N.; Yan, H.; et al. Sampled-Data Control of Networked Autonomous Spacecraft under Sporadic Measurement. *Complex Systems Stability & Control* **2026**, *2*(2), 4. https://doi.org/10.53941/cssc.2026.100007

Received: 11 March 2026
Revised: 15 April 2026
Accepted: 24 April 2026
Published: 29 April 2026

Abstract: This paper researches the sampled-data control problem of networked autonomous spacecraft systems with aperiodic sampling and actuator saturation. Firstly, this paper considers non-differentiable time-varying delays to relax the conventional differentiable assumption and better describe practical networked communication. Subsequently, an improved Lyapunov functional depending on both sampling intervals and delays is constructed to remove the restrictive condition and derive less conservative LMI stability criteria. Especially, considering the physical constraints on actuator outputs in practical spacecraft systems, a sampled-data controller explicitly accounting for actuator saturation is designed, which improves the practical applicability of the proposed control scheme. Finally, a practical example of a flexible spacecraft is provided to verify the effectiveness and rationality of the obtained results.

Keywords: autonomous spacecraft systems; sampled-data control; non-differentiable time-varying delay; actuator saturation; T-S fuzzy modeling

1. Introduction

Over the past decade, autonomous spacecraft systems have attracted sustained research interest due to their critical roles in deep-space exploration, on-orbit servicing, satellite formation flying, and space situational awareness [1,2]. Unlike traditional ground-assisted spacecraft, the attitude dynamics of flexible spacecraft (FS) exhibit strong nonlinearity and rigid-flexible coupling characteristics, which make controller design challenging [3]. The Takagi-Sugeno (T-S) fuzzy model is widely regarded as a mainstream modeling approach for such systems due to its strong nonlinear approximation capability and systematic analysis framework [4]. For instance, robust fuzzy control schemes for flexible spacecraft were developed in [5], where elastic coupling effects were explicitly considered. In [6], a hybrid nonfragile observer-based T-S fuzzy attitude control scheme was proposed for flexible spacecraft subject to input saturation. Moreover, anti-disturbance quantized control based on dynamic event triggers was investigated for flexible spacecraft attitude stabilization in [7]. However, further investigation is still necessary.

Sampled-data control has been widely employed in safety-critical cyber-physical systems since it enables continuous-time plants to be controlled through digital networks while reducing communication and computation burdens. Significant progress has been made in the stability and control of non-uniform sampled-data systems [8]. For instance, a semi-looped-functional-based stability analysis approach was proposed in [9], which provides an effective framework for verifying the stability of sampled-data systems. Furthermore, a sampled-data-based event-triggered fuzzy control scheme for networked systems subject to cyber-attacks was proposed in [10]. On the other hand, actuator saturation is prevalent in many practical aerospace systems, and neglecting this phenomenon may severely degrade transient performance or even lead to instability. To address this issue, actuator-saturation-aware control under multi-rate sampling was studied in [11] to handle sampling and saturation effects jointly. Moreover, sampled-data control approaches have also been investigated for nonlinear systems with actuator nonlinear characteristics [12].

In autonomous spacecraft systems operating over networked environments, non-differentiable time-varying delays, sporadic bounded sampling and packet losses are inevitable, which significantly complicates stability analysis and control design. In addition to deterministic and fuzzy frameworks, semi-Markov jump systems were adopted in [13,14] to characterize system uncertainties. For instance, resilient fuzzy control schemes for nonlinear networked systems under denial-of-service attacks were developed in [15]. Moreover, delay-dependent stability criteria and fuzzy control schemes subject to communication delays were presented in [16,17]. Existing delay-related results for T-S fuzzy systems are generally classified into delay-independent and delay-dependent categories, where the latter can achieve less conservative stability conditions by incorporating delay information [18,19]. In [20], the finite-time fuzzy sampled-data control problem for nonlinear flexible spacecraft with stochastic actuator failures was investigated. In [21], the attitude tracking problem of flexible spacecraft with quantization, actuator dead-zone, and disturbances was addressed by a quantized adaptive fuzzy integral sliding mode control method. However, the study of sampled-data T-S fuzzy systems with non-differentiable delays and bounded sporadic sampling under realistic network environments remains insufficient.

In autonomous spacecraft systems applications, rigid-flexible coupling dynamics, external disturbances, and network-induced uncertainties further increase system complexity. Therefore, the following challenges need to be overcome:

1. How to model networked autonomous spacecraft systems with aperiodic sampling and actuator saturation within the T-S fuzzy framework.
2. How to construct an improved Lyapunov functional depending on both delay information and sampling interval bounds.
3. How to design the fuzzy sampled-data controller with actuator saturation to stabilize the autonomous spacecraft systems.

Inspired by the above discussion, this paper mainly explores the sampled-data control of T-S fuzzy networked control systems with non-differentiable delay and actuator saturation. Compared with the existing work, the highlights of this paper are summarized as follows:

1. Unlike the delay-dependent approaches in [18,19], which assume differentiable delays or impose restrictive delay constraints, this paper develops a networked sampled-data control framework for autonomous spacecraft systems that can accommodate non-differentiable time-varying delays and bounded sporadic sampling within a unified T-S fuzzy modeling framework.
2. A Lyapunov functional depending on both sampling interval and delay information is constructed for the networked autonomous spacecraft system. Compared with the conventional delay-independent and classical delay-dependent approaches in [16,17], the proposed functional effectively integrates delay information and sampling interval bounds, thus reducing the conservatism of the stability criteria.
3. A fuzzy sampled-data controller explicitly considering actuator saturation constraints is proposed in this paper. Compared with the existing sampled-data fuzzy control methods in [11,22], which mainly focus on deterministic sampling or standard H_∞ performance, the proposed controller guarantees the global exponential stability under non-differentiable delays and bounded sporadic sampling.

This paper is organized as follows. Section 2 presents the T-S fuzzy model of the networked flexible spacecraft with non-differentiable time-varying delays and actuator saturation, together with necessary definitions and preliminaries. Section 3 develops the sampled-data stabilization criteria and provides the controller synthesis method based on a Lyapunov functional that incorporates both delay information and sampling interval bounds. Section 4 demonstrates the effectiveness and superiority of the proposed T-S fuzzy networked sampled-data control through a practical example of a flexible spacecraft. Finally, Section 5 concludes this paper. The overall framework of the proposed method is illustrated in Figure 1.

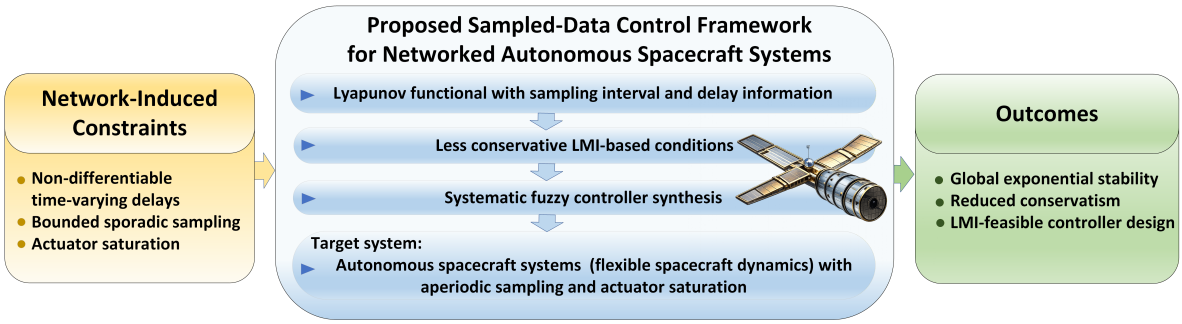

Figure 1. Framework of the proposed sampled-data stabilization method.

2. Model Description and Preliminaries

Based on the FS dynamics described in [20], the attitude kinematics of the system can be characterized by the following positive quaternion representation:

$$\widetilde{\varphi}_0 = \cos\tilde{\delta}/2, \quad \widetilde{\varphi} = \tilde{\gamma}\sin\tilde{\delta}/2,$$

where $\widetilde{\varphi} = [\widetilde{\varphi}_1^{\mathrm{T}}\ \widetilde{\varphi}_2^{\mathrm{T}}\ \widetilde{\varphi}_3^{\mathrm{T}}]^{\mathrm{T}}$ together with $\widetilde{\varphi}_0$ denotes the quaternion representation satisfying the normalization constraint $\sum_{i=1}^{3}\widetilde{\varphi}_i^2 = 1$. Here, $\tilde{\delta}$ denotes the Euler-axis rotation angle and $\tilde{\gamma}$ represents the associated unit vector. Based on this quaternion representation, the attitude kinematics of the flexible spacecraft can be expressed as:

$$\begin{bmatrix}\dot{\widetilde{\varphi}}_0\\ \dot{\widetilde{\varphi}}\end{bmatrix} = \frac{1}{2}\mathscr{H}(\widetilde{\varphi}_0,\widetilde{\varphi})\mathscr{W}, \tag{1}$$

where $\mathscr{W} = [\mathscr{W}_1^{\mathrm{T}}\ \mathscr{W}_2^{\mathrm{T}}\ \mathscr{W}_3^{\mathrm{T}}]^{\mathrm{T}}$ denotes the angular velocity associated with the pitch, roll, and yaw axes. The matrix $\mathscr{H}(\widetilde{\varphi}_0,\widetilde{\varphi})$ is defined as $\mathscr{H}(\widetilde{\varphi}_0,\widetilde{\varphi}) = [-\widetilde{\varphi},(\widetilde{\varphi}_0 I + \mathscr{S}(\widetilde{\varphi}))^{\mathrm{T}}]^{\mathrm{T}}$. Based on this representation, the rigid-flexible coupled dynamics of the spacecraft can be described as:

$$\begin{aligned}&\mathscr{J}\dot{\mathscr{W}}(t) + \zeta^{\mathrm{T}}\ddot{\eta}(t) = -\mathscr{S}(\mathscr{W}(t))(\mathscr{J}\mathscr{W}(t) + \zeta^{\mathrm{T}}\dot{\eta}(t)) + u(t) + \nu(t),\\ &\ddot{\eta}(t) + \mathscr{C}_s\dot{\eta}(t) + \mathscr{K}_s\eta(t) = -\zeta\dot{\mathscr{W}}(t),\end{aligned} \tag{2}$$

where $\mathscr{J} > 0$ represents the inertia matrix of the overall spacecraft system including both rigid bodies and flexible appendages. The matrix ζ characterizes the rigid-flexible coupling effect, while $\eta(t)$ denotes the elastic displacement coordinate. Accordingly, $\dot{\eta}(t)$ and $\ddot{\eta}(t)$ represent the elastic velocity and acceleration of the flexible appendages, respectively. The signal $u(t)$ corresponds to the control input and $\nu(t)$ represents the external disturbance acting on the system. Moreover, $\mathscr{C}_s = \mathrm{diag}\{2\pi_i\mathscr{W}_{ni}\}$ and $\mathscr{K}_s = \mathrm{diag}\{\mathscr{W}_{ni}^2\}$, $i \in \{1,\ldots,N^*\}$, denote the damping and stiffness matrices, respectively.

According to (2), the rigid body motion and elastic vibration are coupled through the terms $\zeta^{\mathrm{T}}\ddot{\eta}(t)$, $\zeta^{\mathrm{T}}\dot{\eta}(t)$ and $\zeta^{\mathrm{T}}\mathscr{W}(t)$. To facilitate the subsequent analysis, a lumped disturbance term is introduced as $\tilde{\nu}(t) = \nu(t) + \zeta^{\mathrm{T}}(\mathscr{C}_s\dot{\eta}(t) + \mathscr{K}_s\eta(t)) - \mathscr{S}(\mathscr{W}(t))\zeta^{\mathrm{T}}\dot{\eta}(t)$, where $\mathscr{S}(\mathscr{W}(t))$ denotes the skew-symmetric matrix associated with the angular velocity vector $\mathscr{W}(t)$, defined as:

$$\mathscr{S}(\mathscr{W}) = \begin{bmatrix}0 & -\mathscr{W}_3 & \mathscr{W}_2\\ \mathscr{W}_3 & 0 & -\mathscr{W}_1\\ -\mathscr{W}_2 & \mathscr{W}_1 & 0\end{bmatrix}.$$

Substituting the above expression into (2) yields the following simplified dynamic model of the flexible spacecraft:

$$(\mathscr{J} - \zeta^{\mathrm{T}}\zeta)\dot{\mathscr{W}}(t) = -\mathscr{S}(\mathscr{W}(t)) + u(t) + \tilde{\nu}(t), \tag{3}$$

where $\tilde{\nu}(t) \in \mathcal{L}_2[0,\mathscr{T})$. Moreover, it is assumed that there exists a positive constant $\hat{\nu}$ such that

$$\int_0^{\mathscr{T}} \tilde{\nu}^{\mathrm{T}}(t)\tilde{\nu}(t)\,\mathrm{d}t \le \hat{\nu}.$$

Define the state variables as $x_i = \mathscr{W}_i$ and $x_{i+3} = \widetilde{\varphi}_i$, $i = 1, 2, 3$. Let $x_{\mathscr{W}} = [x_1, x_2, x_3]^{\mathrm{T}}$, $x_{\widetilde{\varphi}} = [x_4, x_5, x_6]^{\mathrm{T}}$, and $x = [x_{\mathscr{W}}^{\mathrm{T}}, x_{\widetilde{\varphi}}^{\mathrm{T}}]^{\mathrm{T}}$. By combining the attitude kinematics (1) and dynamics (3), a unified nonlinear state-space model is derived. With the quaternion $\widetilde{\varphi}$ and angular velocity $\mathscr{W}$ as outputs, the nonlinear flexible spacecraft dynamics can be rewritten as the following T-S fuzzy form:

Rule i: IF $r_1(t)$ is $\mathcal{N}_{i,1}, \cdots, r_\varrho(t)$ is $\mathcal{N}_{i,\varrho}$, THEN

$$\dot{x}(t) = \mathscr{A}_i x(t) + \mathscr{A}_i^{\bar{\tau}} x(t - \tau(t)) + \mathscr{B}_i \,\mathrm{sat}(u(t)), \tag{4}$$

where $\mathcal{N}_{i,\varrho}$ represents the fuzzy sets, $r_1(t), \ldots, r_\varrho(t)$ denote the premise variables, ϱ denotes the number of fuzzy rules, and $x(t) \in \mathbb{R}^n$ is the state vector of the system. Moreover, the actuator saturation is described by $\mathrm{sat}(u(t)) = u(t) - \phi(u(t))$, where $\phi(u(t))$ characterizes the nonlinear saturation component and satisfies the sector condition $0 \le \phi^{\intercal}(u(t))\big(u(t) - \phi(u(t))\big)$. In addition, the function $\tau(t) : \mathbb{R}_+ \to [0, \bar{\tau}]$ denotes a time-varying delay that is not required to be differentiable. Accordingly, the system matrices A_i, $A_i^{\bar{\tau}}$, and B_i are given by:

$$\mathscr{A}_i = \begin{bmatrix} -(\mathscr{J} - \zeta^{\mathrm{T}}\zeta)^{-1}\mathscr{S}(x_{\mathcal{W}i})\mathscr{J} & 0 \\ \frac{1}{2}\sqrt{1 - \|x_{\widetilde{\varphi}i}\|^2} I & -\frac{1}{2}\mathscr{S}(x_{\mathcal{W}i}) \end{bmatrix},$$
$$\mathscr{A}_i^{\bar{\tau}} = \begin{bmatrix} \mathscr{A}_{i11}^{\bar{\tau}} & 0 \\ 0 & 0 \end{bmatrix}, \quad \mathscr{B}_i = \begin{bmatrix} (\mathscr{J} - \zeta^{\mathrm{T}}\zeta)^{-1} \\ 0 \end{bmatrix},$$

where $\mathscr{A}_{i11}^{\bar{\tau}}$ denotes the delay-state coefficient matrix introduced to characterize the network-induced delay effect in the angular-velocity channel. In this paper, $\mathscr{A}_i^{\bar{\tau}}$ is used to describe the influence of the delayed state $x(t - \tau(t))$ caused by communication and transmission constraints in the networked spacecraft system. The output matrix is taken as $\mathcal{C}_i = I$.

Definition 1. *(Ref. [23]) For the control input $u(t) \in \mathbb{R}^m$, the actuator saturation function $\mathrm{sat}(u(t))$ is defined by*

$$\mathrm{sat}(u(t)) = [\mathrm{sat}(u_1(t)), \mathrm{sat}(u_2(t)), \ldots, \mathrm{sat}(u_m(t))]^T,$$

with

$$\mathrm{sat}(u_k(t)) = \begin{cases} u_{k,\max}, & u_k(t) > u_{k,\max}, \\ u_k(t), & |u_k(t)| \le u_{k,\max}, \\ -u_{k,\max}, & u_k(t) < -u_{k,\max}, \end{cases} \quad k = 1, 2, \ldots, m,$$

where $u_{k,\max} > 0$ is the saturation bound of the k-th actuator.

Remark 1. *Since the flexible spacecraft system is considered in a networked sampled-data environment, communication and transmission delays cannot be neglected in practice. Hence, based on the nominal flexible spacecraft model in [20] and the time-delay approach widely adopted in [24], the delayed-state term $\mathscr{A}_i^{\bar{\tau}} x(t - \tau(t))$ is introduced to describe the network-induced delay effect.*

Remark 2. *Since actuator outputs in practical spacecraft systems are physically bounded in amplitude, actuator saturation should be explicitly considered in the controller design. In this paper, the actuator saturation is described by $\mathrm{sat}(u(t))$, which enables the controller to better capture the practical input constraints. Moreover, by rewriting $\mathrm{sat}(u(t)) = u(t) - \phi(u(t))$, the nonlinear effect caused by actuator saturation can be incorporated into the subsequent Lyapunov-based stability analysis via a sector condition.*

Utilizing the center-average defuzzifier, system (4) can be rewritten as:

$$\dot{x}(t) = \sum_{i=1}^{\varrho} \delta_i(r(t)) \big[\mathscr{A}_i x(t) + \mathscr{A}_i^{\bar{\tau}} x(t - \tau(t)) + \mathscr{B}_i \,\mathrm{sat}(u(t))\big], \tag{5}$$

where $\delta_i(r(t)) = \frac{\vartheta_i(r(t))}{\sum_{k=1}^{\varrho} \vartheta_k(r(t))}$, and $\vartheta_i(r(t)) = \prod_{k=1}^{r} \mathcal{N}_{i,k}(r_k(t))$, with $\mathcal{N}_{i,k}(r_k(t))$ denotes the grade of membership of $r_k(t)$.

Furthermore, the measured output of system (5) is given by

$$y(t) = \sum_{i=1}^{\varrho} \delta_i(r(t)) \mathcal{C}_i x(t_\ell), \quad t \in [t_\ell, t_{\ell+1}), \tag{6}$$

in which $\mathcal{C}_i$ is the output matrix with appropriate dimensions, and t_ℓ denotes the sampling instant satisfying $\{t_\ell\} \in \mathfrak{F}(\eta_0, \eta_1) \triangleq \{t_\ell | \eta_0 \leq t_{\ell+1} - t_\ell \leq \eta_1\}$. The sampled-data control strategy is designed as follows:

Rule j: IF $r_1(t)$ is $\mathcal{N}_{j,1}, \ldots, r_\varrho(t)$ is $\mathcal{N}_{j,\varrho}$, Then

$$u(t) = \mathcal{K}_j y(t_\ell), \quad t \in [t_\ell, t_{\ell+1}), \tag{7}$$

where $\mathcal{K}_j$ represents the control gain matrix. Accordingly, the overall fuzzy sampled-data controller is

$$u(t) = \sum_{j=1}^{\varrho} \delta_j(r(t)) \mathcal{K}_j y(t_\ell), \quad t \in [t_\ell, t_{\ell+1}).$$

Let composite variable $z(t) = \begin{bmatrix} x^{\mathrm{T}}(t) & u^{\mathrm{T}}(t) \end{bmatrix}^{\mathrm{T}}$. By adopting the actuator saturation model $\mathrm{sat}(u(t)) \triangleq u(t) - \phi(u(t))$ in [12], it follows that:

$$\begin{cases} \dot{z}(t) = \sum\limits_{i=1}^{\varrho} \delta_i(r(t)) \sum\limits_{j=1}^{\varrho} \delta_j(r(t)) [\bar{\mathscr{A}}_i z(t) + \bar{\mathscr{A}}_i^{\bar{\tau}} z(t - \tau(t)) + \bar{\mathscr{B}}_\tau \phi(u)], t \neq t_\ell, \\ z(t) = \sum\limits_{i=1}^{\varrho} \sum\limits_{j=1}^{\varrho} \delta_i(r(t)) \delta_j(r(t)) \bar{\gamma}_{i,j} z(t^-), t = t_\ell, \end{cases} \tag{8}$$

where $z(t_\ell^+) = \lim\limits_{m \to 0^+} z(t_\ell + m)$, $z(t_\ell^-) = \lim\limits_{m \to 0^-} z(t_\ell - m)$, $\bar{\mathscr{A}}_i = \begin{bmatrix} \mathscr{A}_i & 0 \\ 0 & 0 \end{bmatrix}$, $\bar{\mathscr{A}}_i^{\bar{\tau}} = \begin{bmatrix} \mathscr{A}_i^{\bar{\tau}} & 0 \\ 0 & 0 \end{bmatrix}$, $\bar{\mathscr{B}}_\tau = -\mathscr{B}_i \begin{bmatrix} I \\ 0 \end{bmatrix}$, and $\bar{\gamma}_{i,j} = \begin{bmatrix} I & 0 \\ \mathcal{K}_j \mathcal{C}_i & 0 \end{bmatrix}$.

Accordingly, the form can be further abbreviated as follows:

$$\begin{cases} \dot{z}(t) = \bar{\mathscr{A}}_i(t) z(t) + \bar{\mathscr{A}}_i^{\bar{\tau}}(t) z(t - \tau(t)) + \bar{\mathscr{B}}_i(t) \phi(t), t \neq t_\ell, \\ z(t) = \bar{\gamma}_{i,j}(t) z(t^-), t = t_\ell, \end{cases} \tag{9}$$

with

$$\bar{\mathscr{B}}_i(t) = \sum_{i=1}^{\varrho} \sum_{j=1}^{\varrho} \delta_i(r(t)) \delta_j(r(t)) \bar{\mathscr{B}}_i, \qquad \bar{\mathscr{A}}_i(t) = \sum_{i=1}^{\varrho} \sum_{j=1}^{\varrho} \delta_i(r(t)) \delta_j(r(t)) \bar{\mathscr{A}}_i,$$

$$\bar{\mathscr{A}}_i^{\bar{\tau}}(t) = \sum_{i=1}^{\varrho} \sum_{j=1}^{\varrho} \delta_i(r(t)) \delta_j(r(t)) \bar{\mathscr{A}}_i^{\bar{\tau}}, \qquad \bar{\gamma}_{i,j}(t) = \sum_{i=1}^{\varrho} \sum_{j=1}^{\varrho} \delta_i(r(t)) \delta_j(r(t)) \bar{\gamma}_{i,j}.$$

Next, a definition required for the subsequent analysis is introduced.

Definition 2. *(Ref. [25]) For a given sampled-data interval $\{t_\ell\} \in \mathfrak{F}(\eta_0, \eta_1)$, the closed-loop system (4) under the controller (7) is said to be globally exponentially stable, if there exist positive constants $\mathcal{M} > 0$ and $\beta > 0$ such that*

$$\|z(t, t_0, \psi)\| \leq \mathcal{M} \|\psi\|_h e^{-\beta(t - t_0)}, \quad t \geq t_0, \tag{10}$$

where $\psi(\delta) = z(t_0 + \delta)$ for $\delta \in [-h, 0]$ denotes the initial function, and $\|\psi\|_h = \sup_{\delta \in [-h, 0]} \|\psi(\delta)\|$.

Remark 3. *Compared with asymptotic stability, global exponential stability provides a stronger characterization of system performance, because it ensures not only the convergence of the closed-loop state to the equilibrium point, but also an explicit exponential decay rate. This is particularly meaningful for the considered networked flexible spacecraft system with non-differentiable delays and actuator saturation.*

3. Main Results

In this section, the stability of the closed-loop networked autonomous spacecraft system under the proposed fuzzy sampled-data controller is analyzed. By constructing a Lyapunov functional incorporating delay and sampling information, LMI-based conditions are derived to ensure global exponential stability.

3.1. Stabilization criterion

In this subsection, the following auxiliary functions and a Lyapunov functional are introduced to establish the stabilization criteria.

For the sampled-data interval $\{t_\ell\} \in \mathfrak{F}(\eta_0, \eta_1)$, the following auxiliary variables are defined:

$$\theta(t) = \frac{1}{t_\ell - t_{\ell-1}}, \quad t \in [t_{\ell-1}, t_\ell), \qquad \xi(t) = \mu^{\iota_{1,0}(t)}, \quad t \in [t_{\ell-1}, t_\ell),$$
$$\iota_{1,0} = \frac{t - t_{\ell-1}}{t_\ell - t_{\ell-1}}, \quad t \in [t_{\ell-1}, t_\ell),$$
$$\iota_{2,0} = \begin{cases} \frac{\xi(t)-1}{\mu-1}, & \mu \neq 1, \\ 1, & \mu = 1, \end{cases} \qquad \iota_{3,0} = \begin{cases} \frac{\theta(t)-\frac{1}{\eta_1}}{\frac{1}{\eta_0}-\frac{1}{\eta_1}}, & \eta_0 < \eta_1, \\ \frac{1}{\eta_0}, & \eta_0 = \eta_1, \end{cases}$$

in which $\mu > 0$ is a design parameter related to the weighting function $\xi(t)$. Define $\iota_{k,1} = 1 - \iota_{k,0}$, $k = 1, 2, 3$. Based on the definitions of $\iota_{2,0}$ and $\iota_{3,0}$, it follows that:

$$\xi(t) = \sum_{j=0}^{1} \iota_{2,j} \mu^{1-j}, \gamma(t) = \sum_{l=0}^{1} \iota_{3,l} \frac{1}{\eta_l}, t \in [t_{\ell-1}, t_\ell). \tag{11}$$

Let

$$\tilde{\iota}_{i,j,l}(t) = \iota_{1,i}(t)\iota_{2,j}(t)\iota_{3,l}(t), i, j, l \in \{0, 1\}. \tag{12}$$

Consider the following Lyapunov function:

$$V(t) = \xi(t) z^{\mathrm{T}}(t) \tilde{\mathcal{F}}(t) z(t), \tag{13}$$

where $\tilde{\mathcal{F}}(t) = \sum_{i=0}^{1} \iota_{1,i}(t) \tilde{\mathcal{F}}_{1-i}$, $t \in [t_{\ell-1}, t_\ell)$, $\tilde{\mathcal{F}}_0 > 0$, $\tilde{\mathcal{F}}_1 > 0$. It is applied to the closed loop system (8) to obtain the following stabilization criteria. And $\eta_{-1} \in \{\eta_0, \eta_1\}$ for $l = 0, 1$.

To handle the actuator saturation in the Lyapunov analysis, introduce a constant matrix $\bar{E}$ with appropriate dimensions and define $\tilde{I}_1 = \begin{bmatrix} 0 & I \end{bmatrix}$. Let the augmented state vector be $z(t) = \begin{bmatrix} x^{\intercal}(t) & u^{\intercal}(t) \end{bmatrix}^{\intercal}$, which implies that $u(t) = \tilde{I}_1 z(t)$. According to the sector-bounded property of $\phi(u(t))$, the following inequality can be obtained $-2\,\phi^{\intercal}(u(t))\,\bar{E}\,[\phi(u(t)) - \tilde{I}_1 z(t)] \geq 0$, which is utilized in the subsequent stability analysis.

Theorem 1. *Given parameters $\eta_0 > 0$, $\eta_1 > 0$, $\omega > 0$ and consider the system (8) over the sampled-data interval $\{t_\ell\} \in \mathfrak{F}(\eta_0, \eta_1)$, the system (9) is globally exponentially stable, if there exist a scalar $\rho > 0$, positive definite matrices $\tilde{\mathcal{F}}_i > 0$ $(i = 0, 1)$, $\tilde{\mathcal{Q}} > 0$, $\tilde{\mathcal{S}} > 0$, and a function $\varpi(t) = e^{2\omega\tau(t)}$, such that*

$$\tilde{\mathcal{F}}_i \geq \tilde{\mathcal{Q}}, \quad i = 0, 1, \tag{14}$$

$$\Xi_{i,j,l}(t) = \begin{bmatrix} \Xi^1_{i,j,l}(t) & \Xi^2_{i,j,l}(t) & \Xi^3_{i,j,l}(t) \\ * & -\varpi(t)\sigma\tilde{\mathcal{Q}} & 0 \\ * & * & -2\tilde{\mathcal{S}} \end{bmatrix} < 0, \tag{15}$$

$$\begin{bmatrix} -\sigma\tilde{\mathcal{F}}_1 & (I + \bar{\gamma}_{i,j}\tilde{\mathcal{F}}_0) \\ * & -\tilde{\mathcal{F}}_0 \end{bmatrix} < 0, \tag{16}$$

where

$$\Xi^1_{i,j,l}(t) = \sigma^{1-j}\Big(\Pi_{i,l}(t) + \varpi(t)e^{2\omega\bar{\tau}}\tilde{\mathcal{F}}_{1-i}\Big),$$
$$\Xi^2_{i,j,l}(t) = \sigma^{1-j}\tilde{\mathcal{F}}_{1-i}\bar{\mathscr{A}}_i^{\bar{\tau}}(t),$$
$$\Xi^3_{i,j,l}(t) = \tilde{I}_1^{\mathrm{T}}\tilde{E}^{\mathrm{T}} - \tilde{\mathcal{F}}_{1-i},$$
$$\Pi_{i,l}(t) = \left[\frac{\ln\sigma}{\eta_l} + 2\omega\right]\tilde{\mathcal{F}}_{1-i} + \mathrm{sym}\big\{\tilde{\mathcal{F}}_{1-i}\bar{\mathscr{A}}_i(t)\big\} + \frac{1}{\eta_l}\big[\tilde{\mathcal{F}}_1 - \tilde{\mathcal{F}}_0\big].$$

Proof. See Appendix A. □

Remark 4. *Compared with [9, 26], which mainly consider differentiable time-varying delays or deterministic sampling structures, and [18, 22], where delay-dependent criteria rely on smoothness assumptions or restrictive*

delay constraints, the proposed criteria provide a more general framework by accommodating non-differentiable time-varying delays and bounded sporadic sampling, thereby reducing the conservatism of the stability conditions.

Remark 5. *It should be noted that the conditions (15) and (16) in above Theorem 1 is a stable and discriminant condition, but it cannot find the gain matrix. To address this issue, Theorem 2 presents a controller condition for determining the control gain matrix.*

3.2. Controller design

Theorem 2. *Given parameters $\eta_0 > 0$, $\eta_1 > 0$, controller gain is $K_i = Y_1^{-1}\tilde{K}_i$, and consider system (8) over the sampled-data interval $\{t_\ell\} \in \mathfrak{F}(\eta_0, \eta_1)$, the system (9) under the sampled-data controller (7) is globally exponentially stable, if conditions (14) and (15) hold and there exist scalars $\sigma > 0$, $\kappa > 0$ and positive definite matrices $\widetilde{P}_i$, $\widetilde{Q}$, Y_i, and $\widetilde{K}_i$ such that*

$$\begin{bmatrix} -\sigma\tilde{P}_1 & \bar{\gamma}_0\tilde{\mathcal{F}}_0 + \mathcal{I}_0^{\mathrm{T}}\mathcal{C}_i^{\mathrm{T}}[\kappa\tilde{\mathcal{K}}_i^{\mathrm{T}} \quad 0 \quad \tilde{\mathcal{K}}_i^{\mathrm{T}}] \\ * & -\tilde{\mathcal{F}}_0 \end{bmatrix} < 0, \tag{17}$$

where

$$\tilde{\mathcal{F}}_0 = \begin{bmatrix} \mathcal{Y}_0 & \kappa\tilde{\mathcal{Y}}_1 \\ * & \mathcal{Y}_1 \end{bmatrix}, \quad \tilde{\mathcal{Y}}_1 = \begin{bmatrix} \mathcal{Y}_1 \\ 0 \end{bmatrix}.$$

Proof. Let $\tilde{\mathcal{F}}_0 = \begin{bmatrix} \mathcal{Y}_0 & \kappa\tilde{\mathcal{Y}}_1 \\ * & Y_1 \end{bmatrix}$ with $\tilde{\mathcal{Y}}_1 = \begin{bmatrix} \mathcal{Y}_1 \\ 0 \end{bmatrix}$. Substituting it into (17), it is clear that (17) is equivalent to condition (16) in Theorem 1, which completes the proof. □

Remark 6. *The condition (15) in Theorem 1 relates to time t, which is mainly affected by the membership degree of the model. The processing technique of this inequality is mainly based on reference [19], on which it can be easily solved, due to space limitations, the detailed derivation is omitted.*

4. Simulation Results

In this section, a practical example of a flexible spacecraft is provided to illustrate the effectiveness of the proposed T-S fuzzy networked sampled-data control scheme.

Example 1. *Consider a fuzzy FS system whose parameters are adopted from [20]. The system matrices $\mathcal{A}_i$, $\mathcal{B}_i$ and $\mathcal{C}_i$ are defined according to (4). In this example, the T-S fuzzy model consists of $\varrho = 7$ rules.*

The principal inertia matrix is given by:

$$\mathscr{J} = \begin{bmatrix} 350 & 3 & 4 \\ * & 270 & 10 \\ * & * & 190 \end{bmatrix} \mathrm{kg}\cdot\mathrm{m}^2,$$

and the coupling matrix

$$\zeta = \begin{bmatrix} 6.45637 & 1.27814 & 2.15629 \\ 1.25619 & 0.91756 & 1.67264 \\ 0 & 10 & 190 \end{bmatrix} \mathrm{kg}^{1/2}\cdot\mathrm{m},$$

and other parameters are chosen from [27]. For numerical simulation, the total simulation time is set to 30 s and the integration step size is chosen as $dt = 10^{-3}$. The initial condition is taken as $x_0 = [-1.27\ 0.35\ 1.2\ -0.25\ 1.5\ 0.75]^T$. To characterize the network-induced delay effect, the non-differentiable time-varying delay is selected as $h(t) = |\cos(0.8t)| + 1.2|\sin(2t)|$, whose evolution is shown in Figure 2. Since the adopted delay function contains absolute-value terms, it is non-differentiable at some instants, which is consistent with the considered networked communication scenario. In addition, the aperiodic sampling sequence $\{t_\ell\}$ is randomly generated under the constraint $\eta_0 \le t_{\ell+1} - t_\ell \le \eta_1$, where $\eta_0 = 0.02$ and $\eta_1 = 0.25$. To ensure reproducibility of the simulation results, the random seed is fixed in the numerical implementation. The control signal is updated only at the sampling instants and held constant over each interval $[t_\ell, t_{\ell+1})$.

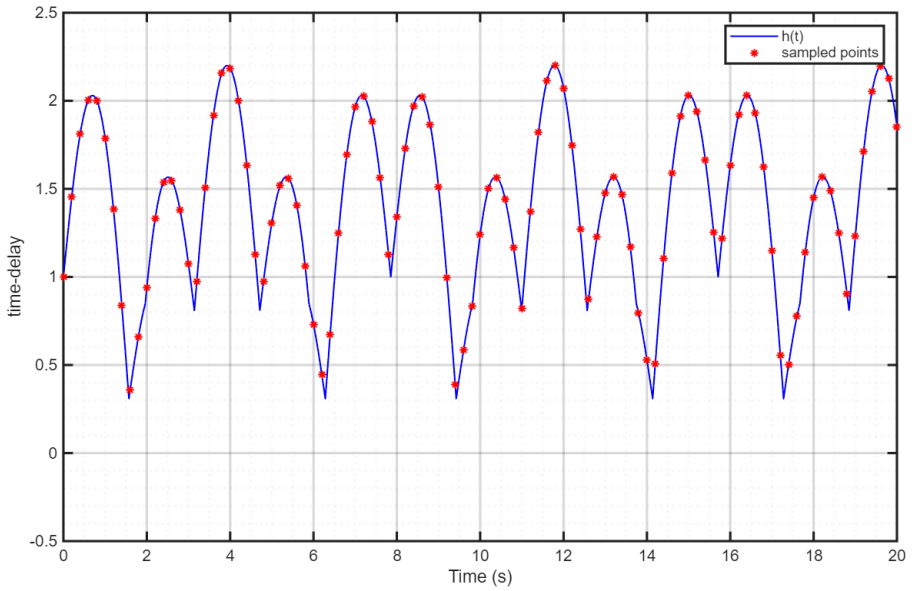

Figure 2. Evolutionary trajectory curve with non-differentiable delay.

In the expression of the lumped disturbance $\tilde{\nu}(t)$, the term $\nu(t)$ represents external disturbances, such as gravitational torques or aerodynamic effects, and is assumed to take the following form:

$$\nu(t) = 10^{-1} \cdot \begin{bmatrix} -1.6 + 2\cos(0.16t) - 1.1\cos(0.4t) \\ 3.5 + 1.5\sin(0.16t) - 2.0\cos(0.4t) \\ -1.6 + 2.0\sin(0.16t) - 1.8\sin(0.4t) \end{bmatrix} \mathrm{N} \cdot \mathrm{m}.$$

The state trajectories of the fuzzy FS described by (4) without control, under the initial condition $x_0 = [-1.27\ 0.35\ 1.2\ -0.25\ 1.5\ 0.75]^{\mathrm{T}}$, are shown in Figure 3. It can be observed that the open-loop system is unstable. Motivated by this observation, the extended dissipative performance of the system will be investigated using a secure fuzzy sampled-data control strategy.

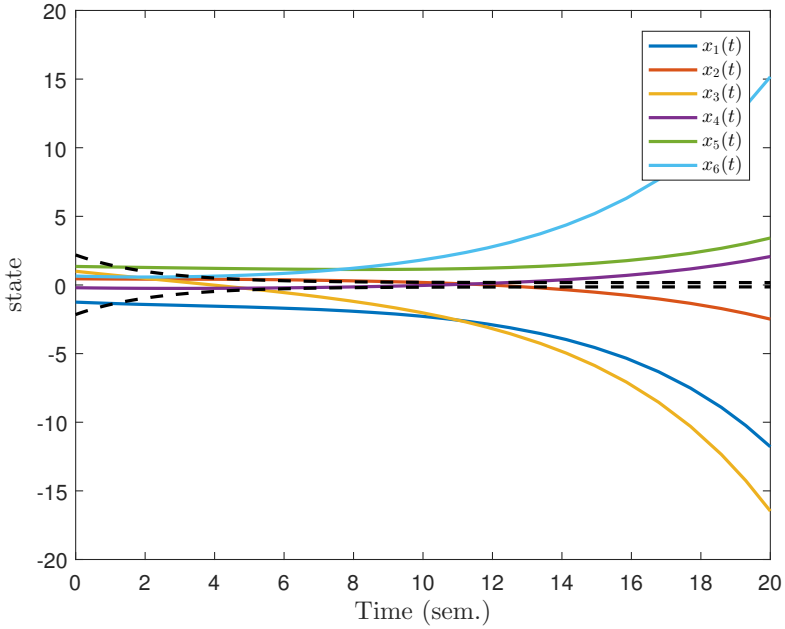

Figure 3. The state trajectory of the open-loop system.

The parameters are chosen as $\eta_0 = 0.02$, $\eta_1 = 0.25$, $\mu = 0.09703$, $\sigma = 0.00155$. By solving the conditions in Theorem 2, the following control gain matrices are obtained for system (4) under non-differentiable delay and actuator saturation:

$$K_1 = \begin{bmatrix} -146.17 & 90.81 & 195.16 & -214.11 & 71.56 & 203.18 \\ 93.34 & -97.10 & 54.69 & -52.67 & -4.17 & 58.3123 \\ 3.35 & 36.23 & 421.29 & 56.41 & -16.13 & -54.62 \end{bmatrix},$$

$$K_2 = \begin{bmatrix} -145.29 & 88.44 & 197.06 & -212.88 & 69.61 & 201.73 \\ 94.87 & -99.08 & 56.90 & -49.41 & -6.90 & 54.87 \\ 2.79 & 37.56 & 420.99 & 56.23 & -15.20 & -53.24 \end{bmatrix},$$

$$K_3 = \begin{bmatrix} -145.29 & 88.44 & 197.06 & -212.88 & 69.61 & 201.73 \\ 94.87 & -99.08 & 56.90 & -49.41 & -6.90 & 54.87 \\ 2.79 & 37.56 & 420.99 & 56.23 & -15.20 & -53.24 \end{bmatrix},$$

$$K_4 = \begin{bmatrix} -148.22 & 90.09 & 197.37 & -214.98 & 70.44 & 204.49 \\ 95.87 & -102.37 & 56.38 & -49.26 & -8.82 & 55.99 \\ 2.75 & 37.85 & 426.97 & 53.90 & -14.47 & -51.60 \end{bmatrix}.$$

$$K_5 = \begin{bmatrix} -136.96 & 72.20 & 201.07 & -184.07 & 49.27 & 178.17 \\ 105.73 & -118.91 & 63.32 & -1.31 & -36.87 & 13.89 \\ -1.31 & 44.22 & 411.99 & 37.51 & -4.39 & -35.87 \end{bmatrix},$$

$$K_6 = \begin{bmatrix} -149.46 & 90.63 & 198.43 & -216.59 & 70.83 & 205.94 \\ 96.62 & -103.71 & 56.96 & -49.40 & -9.53 & 56.22 \\ 2.62 & 38.47 & 431.54 & 53.62 & -14.12 & -51.20 \end{bmatrix},$$

$$K_7 = \begin{bmatrix} -143.78 & 83.12 & 204.02 & -216.73 & 68.01 & 202.64 \\ 100.91 & -103.86 & 61.69 & -43.41 & -11.85 & 46.43 \\ 1.06 & 40.57 & 425.43 & 58.53 & -14.68 & -53.51 \end{bmatrix}.$$

The actuator responses under the prescribed saturation bounds $u_{k,\max} = 2$, $k = 1, 2, 3$, *are illustrated in Figure 4, where* $u_{k,\max}$ *denotes the saturation bound of the* k*-th actuator. From Figure 4, it is seen that the control inputs are always confined within the prescribed bounds, showing that the actuator saturation constraints are properly respected. Furthermore, Figure 5 depicts the state trajectories of the closed-loop system obtained by using the above state feedback gain matrices. As can be observed, all state variables converge to the equilibrium point in a stable manner. These results confirm that the proposed fuzzy sampled-data controller (7) can effectively stabilize the closed-loop fuzzy FS (8) under actuator saturation constraints.*

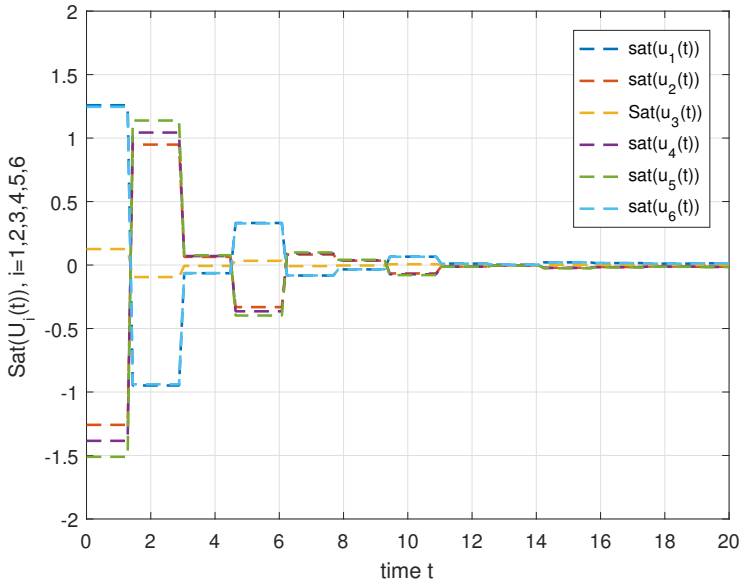

Figure 4. The trajectory of saturated control input signal.

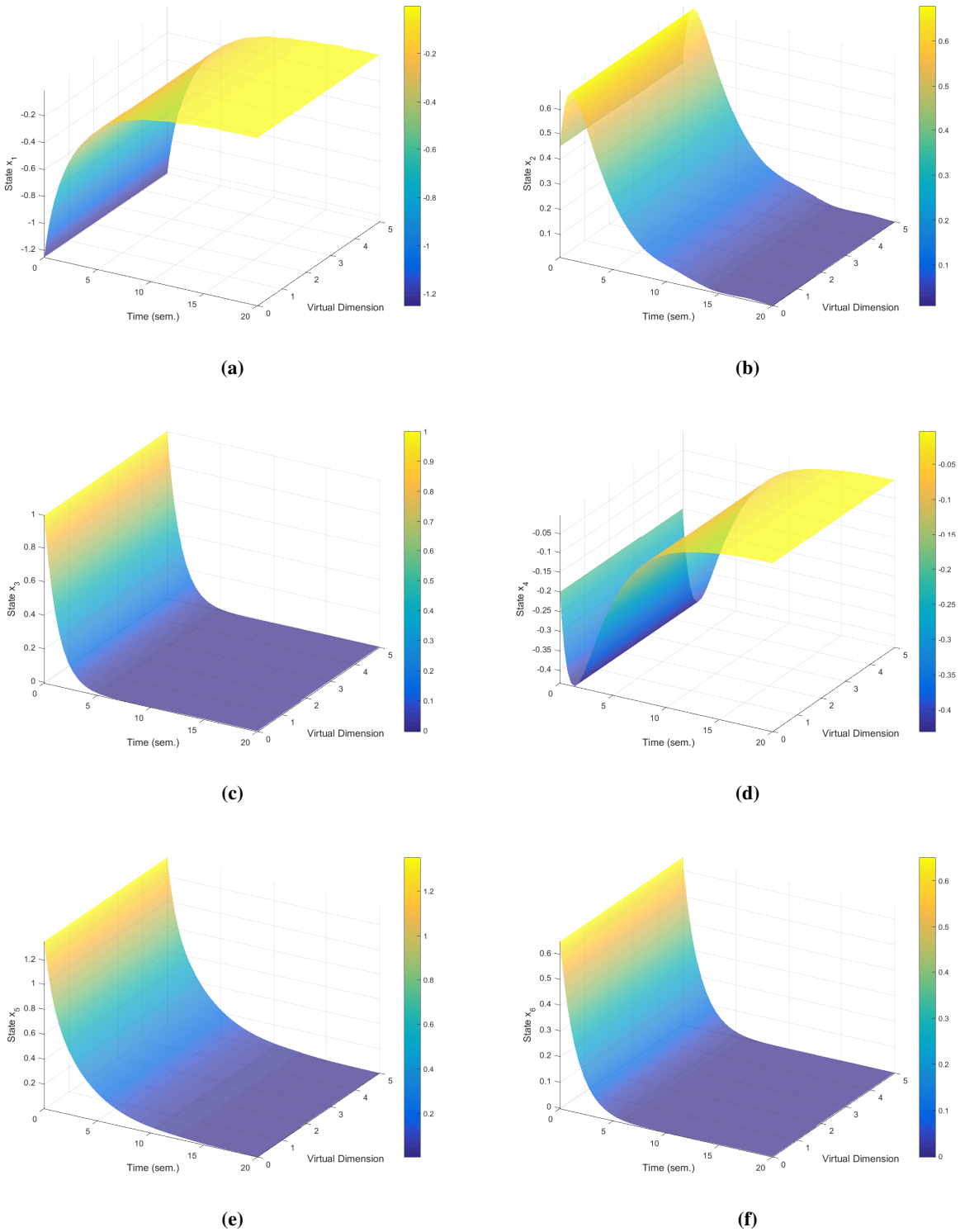

Figure 5. (**a**)–(**f**) The state trajectory of the closed-loop system (8).

To further verify the effectiveness of the proposed method, comparative simulations are conducted with the method in [20] under the same simulation settings. The main results are summarized in Table 1. It should be emphasized that the proposed method is developed for a more practical control framework, where non-differentiable time-varying delays, aperiodic sampling, and actuator saturation are explicitly taken into account, while the method in [20] does not explicitly address actuator saturation or network-induced delay effects. As shown in Table 1, under these more general conditions, the proposed method still achieves comparable convergence performance, together with a smaller peak state norm and terminal state norm.

Table 1. Comparison of control performance

Method	Settling Time (s)	Peak State Norm	Peak Control Norm	Terminal State Norm
[20]	15.754	3.0543	6.6793	0.27169
This paper	14.939	2.9785	6.9282	0.23347

5. Conclusions

In this paper, the sampled-data control problem for networked autonomous spacecraft systems subject to aperiodic sampling and actuator saturation has been investigated. To ensure the global exponential stability of the closed-loop system under bounded sporadic sampling, a fuzzy sampled-data controller has been developed, and a new sufficient stability condition has been established by constructing a Lyapunov functional incorporating both delay information and sampling interval bounds. Tractable LMI-based criteria have been derived to facilitate controller synthesis, and MATLAB can be utilized to verify the feasibility of the proposed approach. The results indicate that stability can be achieved without requiring the differentiability of time-varying delays or imposing restrictive delay constraints. Finally, the effectiveness and practicality of the proposed method are demonstrated through a practical example of a flexible spacecraft.

Author Contributions

Y.D.: conceptualization, methodology, and writing—original draft preparation; N.Y.: software, validation, and data curation; H.S.: supervision, methodology, and writing—reviewing and editing; H.Y.: supervision, funding acquisition, and writing—reviewing and editing; Y.Z.: visualization and investigation; K.D.: validation, formal analysis, and writing—reviewing and editing. All authors have read and agreed to the published version of the manuscript.

Funding

This work was supported in part by the National Natural Science Foundation of China under Grant 62403006, and Grant 12501609, and in part by the Anhui Provincial Natural Science Foundation under Grant 2408085QF184, Grant 250808QA035, and Grant 2023AH010011.

Institutional Review Board Statement

Not applicable.

Informed Consent Statement

Not applicable.

Data Availability Statement

Not applicable.

Conflicts of Interest

The authors declare no conflict of interest.

Use of AI and AI-Assisted Technologies

No AI tools were utilized for this paper.

Appendix A. Proof of Theorem 1

Proof. By Schurs complement lemma, condition (16) is equivalent to:

$$(I+\bar{\gamma}_{i,j})^{\mathrm{T}}(\tilde{I}+\bar{\gamma}_{i,j}) \leq \sigma\tilde{\mathcal{F}}_1. \tag{A1}$$

Define $\tilde{\Omega}(t) = e^{2\omega(t-t_0)}V(t)$, and let $\alpha_{1,1} = \max_{i=1,2}\{\alpha_{\max}(\tilde{\mathcal{F}}_i)\}$, $\alpha_{1,2} = \min_{i=1,2}\{\alpha_{\min}(\tilde{\mathcal{F}}_i)\}$. For any given $\varepsilon > 0$, the feasibility of the following inequality is proven below:

$$\tilde{\Omega}(t) < \varepsilon\alpha_{1,1}\|z_{t_0}\|^2, t \in [t_{\ell-1}, t_\ell). \tag{A2}$$

From the definition of $\tilde{W}(t)$, it follows that (A2) holds for $\ell = 0$. Assume that for some $\ell \in \mathbb{N}_0$,

$$\tilde{\Omega}(t) < \varepsilon\alpha_{1,1}\|z_{t_0}\|^2, t \in [-\overline{\tau}, t_\ell). \tag{A3}$$

Then, for $t \in [t_\ell, t_{\ell+1})$,

$$\tilde{\Omega}(t) < \varepsilon\alpha_{1,1}\|z_{t_0}\|^2, t \in [-t_\ell, t_{\ell+1}). \tag{A4}$$

From (A1), it follows that:

$$\begin{aligned}
\tilde{\Omega}(t_\ell) &= \exp[2\omega(t_\ell - t_0)]\xi(t_\ell)z^\top(t_\ell)\tilde{\mathcal{F}}(t_\ell)z(t_\ell) \\
&= \exp[2\omega(t_\ell - t_0)]z^\top(t_\ell^-)(I + \bar{\gamma}_{i,j})^\top\tilde{\mathcal{F}}_0(I + \bar{\gamma}_{i,j})z(t_\ell^-) \\
&\leq \sigma\exp[2\omega(t_\ell - t_0)]z^\top(t_\ell^-)\tilde{\mathcal{F}}_1 z(t_\ell^-) \\
&= \exp[2\omega(t_\ell - t_0)]\xi(t_\ell^-)z^\top(t_\ell^-)\tilde{\mathcal{F}}(t_\ell^-)z(t_\ell^-) \\
&= \tilde{\Omega}(t_\ell^-).
\end{aligned} \tag{A5}$$

Suppose that (A4) does not hold. Then there exists $t_c \in [t_\ell, t_{\ell+1})$ such that:

$$\tilde{\Omega}(t_*) = \varepsilon\alpha_{1,1}\|z_{t_0}\|^2, \tilde{\Omega}(t) < \varepsilon\alpha_{1,1}\|z_{t_0}\|^2, t \in [t_0 - \overline{\tau}, t_c), \tag{A6}$$

and

$$\tilde{\Omega}(t_c) \geq 0. \tag{A7}$$

From (A6), it follows that:

$$\tilde{\Omega}(t) > \tilde{\Omega}(t_c - \tau(t_c)).$$

Using $\xi(t) \geq \underline{\sigma}$, and condition (14), it follows that:

$$0 \leq \varpi(t)[\exp(2\omega\bar{\tau})\xi(t_c)z^\top(t_c)\tilde{\mathcal{F}}(t_c)z(t_c) - \underline{\sigma}z^\top(t_c - \tau(t_c))]\tilde{\mathcal{Q}}z(t_c\tau(t_c)). \tag{A8}$$

For $t \in [t_\ell, t_{\ell+1})$, along the trajectory of the closed-loop system (8), the derivative of $\tilde{\Omega}(t)$ satisfies:

$$\begin{aligned}
\dot{\tilde{\Omega}}(t) =& \xi(t)\exp\big(2\omega(t - t_0)\big)\Big[z^\top(t)\Big(\big(2\omega + \ln\sigma\theta(t)\big)\tilde{\mathcal{F}}(t) \\
&+ \theta(t)(\tilde{\mathcal{F}}_1 - \tilde{\mathcal{F}}_0) + \mathrm{sym}\left\{\tilde{\mathcal{F}}(t)\bar{\mathscr{A}}_i(t)\right\}\Big)z(t) \\
&+ 2z^\top(t)\tilde{\mathcal{F}}(t)\bar{\mathscr{A}}_i^{\bar{\tau}}(t)z(t - \tau(t))\Big].
\end{aligned} \tag{A9}$$

Substituting (A8) and (A9) for $t = t_c$, and using $-2\phi^\top(u)\bar{E}[\phi(u) - \tilde{I}_1 z(t)] \geq 0$, yields:

$$\dot{\tilde{\Omega}}(t) \leq \exp\big(2\omega(t - t_0)\big)\sum_{i=0}^{1}\sum_{j=0}^{1}\sum_{l=0}^{1}\tilde{\iota}_{i,j,l}(t_c)\Xi_{i,j,l}(t_c). \tag{A10}$$

By virtue of condition (15), it can be clearly found that $\dot{\tilde{\Omega}}(t) \leq 0$ is obviously in contradiction with (A7). Thus, for any $\varepsilon > 0$, it holds that

$$\tilde{\Omega}(t) \leq \alpha_{1,1}\|z_{t_0}\|_{\bar{\tau}}, \quad t \geq t_0.$$

Consequently,

$$\|z(t)\| \leq \sqrt{\frac{\alpha_{1,1}\sigma}{\alpha_{1,2}}}\|z_{t_0}\|_{\bar{\tau}}\exp\big(-\omega(t - t_0)\big). \tag{A11}$$

Therefore, the closed-loop system is exponentially stable under the sampled-data controller. The proof is completed. □

References

1. Fear, A.; Lightsey, E. Autonomous rendezvous and docking implementation for small satellites using model predictive control. *J. Guid. Control Dyn.* **2024**, *47*, 539–547.
2. Wang, B.; Li, S.; Mu, J.; et al. Research advancements in key technologies for space-based situational awareness. *Space Sci. Technol.* **2022**, *2022*, 9802793.
3. Zhang, L.; Ren, H.; Fan, W.; et al. Dynamic modeling and trajectory optimization for the rigid-flexible coupled spacecraft with the free-floating manipulator and solar panels. *Appl. Math. Model.* **2025**, *137*, 115706.
4. Tanaka, K.; Sugeno, M. Stability analysis and design of fuzzy control systems. *Fuzzy Sets Syst.* **1992**, *45*, 135–156.
5. Liu, Q.; Liu, M.; Duan, G. Adaptive fuzzy backstepping control for attitude stabilization of flexible spacecraft with signal quantization and actuator faults. *Sci. China Inf. Sci.* **2021**, *64*, 152205.
6. Lyu, B.; Liu, C.; Yue, X. Hybrid nonfragile intermediate observer-based T-S fuzzy attitude control for flexible spacecraft with input saturation. *Aerosp. Sci. Technol.* **2022**, *128*, 107753.
7. Zhu, C.; Sun, H.; Hou, L. Anti-disturbance attitude quantized control of flexible spacecraft via a triggering and quantization joint dynamic event-triggered mechanism. *Aerosp. Sci. Technol.* **2023**, *136*, 108191.
8. Zhang, X.; Han, Q.; Ge, X.; et al. Sampled-data control systems with non-uniform sampling: A survey of methods and trends. *Annu. Rev. Control* **2023**, *55*, 70–91.
9. Sheng, Z.; Lin, C.; Xu, S. A semi-looped-functional for stability analysis of sampled-data systems. *IEEE/CAA J. Autom. Sin.* **2023**, *10*, 1332–1335.
10. Song, X.; Zhang, Q.; Song, S.; et al. Sampled-data-based event-triggered fuzzy control for PDE systems under cyberattacks. *IEEE Trans. Fuzzy Syst.* **2022**, *30*, 2693–2705.
11. Ferrante, F.; Sanfelice, R.; Tarbouriech, S. Control design under actuator saturation and multi-rate sampling. *Automatica* **2023**, *148*, 110767.
12. Chen, Y.; Wang, Z.; Shen, B.; et al. Local stabilization for multiple input-delay systems subject to saturating actuators: The continuous-time case. *IEEE Trans. Autom. Control* **2022**, *67*, 3090–3097.
13. Wu, X.; Shi, P.; Tang, Y.; et al. Stability analysis of semi-Markov jump stochastic nonlinear systems. *IEEE Trans. Autom. Control* **2022**, *67*, 2084–2091.
14. Wu, X.; Tang, Y.; Mao, S.; et al. Stability analysis and stabilization of semi-Markov jump linear systems with unavailable sojourn-time information. *Sci. China Inf. Sci.* **2024**, *67*, 172201.
15. Zhao, N.; Shi, P.; Xing, W.; et al. Resilient adaptive event-triggered fuzzy tracking control and filtering for nonlinear networked systems under denial-of-service attacks. *IEEE Trans. Fuzzy Syst.* **2022**, *30*, 3191–3201.
16. Zeng, H.; Zhu, Z.; Peng, T.; et al. Robust tracking control design for a class of nonlinear networked control systems considering bounded package dropouts and external disturbance. *IEEE Trans. Fuzzy Syst.* **2024**, *32*, 3608–3617.
17. Cai, X.; Shi, K.; She, K.; et al. New results for T-S fuzzy systems with hybrid communication delays. *Fuzzy Sets Syst.* **2022**, *438*, 1–24.
18. Lian, Z.; He, Y.; Zhang, C.-K.; et al. Robust H_∞ control for T-S fuzzy systems with state and input time-varying delays via delay-product-type functional method. *IEEE Trans. Fuzzy Syst.* **2019**, *27*, 1917–1930.
19. Chen, B.; Wang, Z.; Zhao, F.; et al. Fault-tolerant event-triggered sampled-data fuzzy control for nonlinear delayed parabolic PDE systems. *IEEE Trans. Fuzzy Syst.* **2024**, *32*, 6460–6471.
20. Sun, G.; Xu, S.; Li, Z. Finite-time fuzzy sampled-data control for nonlinear flexible spacecraft with stochastic actuator failures. *IEEE Trans. Ind. Electron.* **2017**, *64*, 3851–3861.
21. Li, A.; Liu, M.; Cao, X.; et al. Adaptive quantized sliding mode attitude tracking control for flexible spacecraft with input dead-zone via takagi-sugeno fuzzy approach. *Inf. Sci.* **2022**, *587*, 746–773.
22. Yan, S.; Gu, Z.; Ding, L.; et al. Weighted memory H_∞ stabilization of time-varying delayed Takagi-Sugeno fuzzy systems. *IEEE Trans. Fuzzy Syst.* **2024**, *32*, 337–342.
23. Seuret, A.; Tarbouriech, S. Data-driven event-triggering mechanism for linear systems subject to input saturation. *Eur. J. Control* **2024**, *80*, 101045.
24. Liu, K.; Selivanov, A.; Fridman, E. Survey on time-delay approach to networked control. *Annu. Rev. Control* **2019**, *48*, 57–79.
25. Fridman, E. Introduction to Time-Delay Systems: Analysis and Control. *Berlin, Germany: Springer.* **2014**
26. Xu, J.; Niu, Y.; Lam, H. Nonperiodic multirate sampled-data fuzzy control of singularly perturbed nonlinear systems. *IEEE Trans. Fuzzy Syst.* **2023**, *31*, 2891–2903.
27. Zhu, Q.; Kumar, S.; Raja, R.; et al. Extended dissipative analysis for aircraft flight control systems with random nonlinear actuator fault via non-fragile sampled-data control. *J. Franklin Inst.* **2019**, *356*, 8610–8624.